
Adaptive Depth Networks with Skippable Sub-Paths

Woochul Kang

Department of Embedded Systems
Incheon National University
Yeonsu-gu, Incheon, South Korea, 22012
wchkang@inu.ac.kr

Abstract

Predictable adaptation of network depths can be an effective way to control inference latency and meet the resource condition of various devices. However, previous adaptive depth networks do not provide general principles and a formal explanation on why and which layers can be skipped, and, hence, their approaches are hard to be generalized and require long and complex training steps. In this paper, we present a practical approach to adaptive depth networks that is applicable to various networks with minimal training effort. In our approach, every hierarchical residual stage is divided into two sub-paths, and they are trained to acquire different properties through a simple self-distillation strategy. While the first sub-path is essential for hierarchical feature learning, the second one is trained to refine the learned features and minimize performance degradation if it is skipped. Unlike prior adaptive networks, our approach does not train every target sub-network in an iterative manner. At test time, however, we can connect these sub-paths in a combinatorial manner to select sub-networks of various accuracy-efficiency trade-offs from a single network. We provide a formal rationale for why the proposed training method can reduce overall prediction errors while minimizing the impact of skipping sub-paths. We demonstrate the generality and effectiveness of our approach with convolutional neural networks and transformers.

1 Introduction

Modern deep neural networks such as convolutional neural networks (CNNs) and transformers [1] provide state-of-the-art performance at high computational costs, and, hence, lots of efforts have been made to leverage those inference capabilities in various resource-constrained devices. Those efforts include compact architectures [2, 3], network pruning [4, 5], weight/activation quantization [6], knowledge distillation [7], to name a few. However, those approaches provide static accuracy-efficiency trade-offs, and, hence, it is infeasible to deploy one single model to meet devices with all kinds of resource-constraints.

There have been some attempts to provide predictable adaptability to neural networks by exploiting the redundancy in either network depths [8, 9], widths [10, 11], or both [12, 13]. However, one major difficulty with prior adaptive networks is that they are hard to train and require significantly longer training time than non-adaptive networks. For example, most adaptive networks select a fixed number of sub-networks of varying depths or width, and train them iteratively, mostly through self-distilling knowledge from the largest sub-network (also referred to as the *super-net*) [10, 11, 13, 14]. However, this exhaustive self-distillation takes long time and can generate conflicting training objectives for different parameter-sharing sub-networks, potentially resulting in worse performance [15, 16]. Moreover, unlike width-adaptation networks, there is no established principle for adapting depths since the impact of skipping individual layers has not been formally defined.

In this work, we introduce an architectural pattern and training method for adaptive depth networks that is generally applicable to various networks, e.g., CNNs and transformers. In the proposed

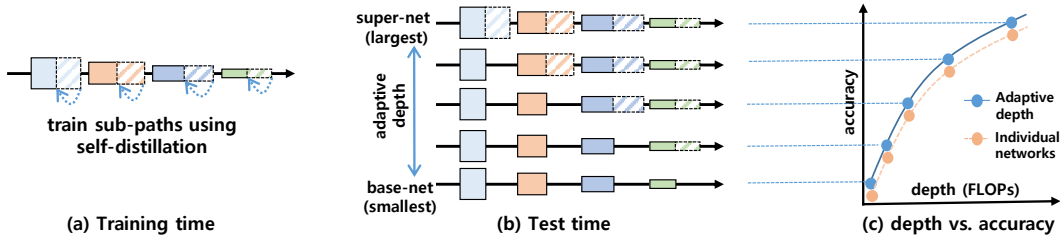


Figure 1: (a) During training, each residual stage of a network is divided into two sub-paths. The layers in the second sub-paths are optimized to minimize performance degradation even if they are skipped. (b) At test time, we can instantly select 2^{N_r} parameter-sharing sub-networks from a single network by systematically skipping the last half layers of N_r residual stages. (c) The sub-networks selected from a single network form a better Pareto frontier compared to individual networks.

adaptive depth networks, every residual stage is divided into two sub-paths and the sub-paths are trained to have different properties. While the first sub-paths are mandatory for hierarchical feature learning, the second sub-paths are optimized to incur minimal performance degradation even if they are skipped. In order to enforce this property of the second sub-paths, we propose a simple self-distillation strategy, in which only the largest sub-network (or, *super-net*) and the smallest sub-network (or, *base-net*) are exclusive used as a teacher and a student, respectively, as shown in Figure-1-(a). The proposed self-distillation strategy does not require exhaustive training of every target sub-network, resulting in significantly shorter training time than prior adaptive networks. Nevertheless, at test time, sub-networks with various depths can be selected instantly from a single network by connecting these sub-paths in a combinatorial manner, as shown in Figure 1-(b). Further, these sub-networks with varying depths outperform individually trained non-adaptive networks due to the regularization effect, as shown in Figure 1-(c).

In Section 3, we discuss the details of our architectural pattern and training algorithm, and show formally that the selected sub-paths trained with our self-distillation strategy are optimized to reduce prediction errors while minimally changing the level of input features. In Section 4, we empirically demonstrate that our adaptive depth networks outperform counterpart individual networks, both in CNNs and vision transformers, and achieve actual inference acceleration and energy-saving.

To authors’ best knowledge, this is the first approach to adaptive networks that provides a general principle and theoretic basis for how depth adaptation can be supported with minimal performance degradation and training effort. This allows us to avoid typical exhaustive training of target sub-networks and instead construct sub-networks of varying depths from specifically trained sub-paths. We anticipate these advances will facilitate future research and applications of adaptive networks.

2 Related Work

Adaptive Networks: In most adaptive networks, parameter-sharing sub-networks are instantly selected by adjusting either widths, depths, or resolutions [8, 10, 11, 17, 13, 15, 18, 12, 19]. For example, slimmable neural networks adjust channel widths of CNN models on the fly for accuracy-efficiency trade-offs and they exploit switchable batch normalization to handle multiple sub-networks [10, 20, 11]. Transformer-based adaptive depth networks have been proposed for language models to dynamically skip some of the layers during inference [13, 9]. However, in these adaptive networks, every target sub-network with varying widths or depths need to be trained explicitly, incurring significant training overheads and potential conflicts between sub-networks.

Dynamic Networks: Dynamic networks [21] are another class of adaptive networks that exploit additional control networks or decision gates for input-dependent adaptation of CNN models [22, 23, 24, 25, 26] and transformers [27, 28, 29, 30]. In particular, most dynamic networks for depth-adaptation have some kinds of decision gates at every layers (or blocks) that determine if the layers can be skipped [31, 22, 32, 33]. These approaches are based on the thought that some layers can be skipped on ‘easy’ inputs. However, the learned policy for skipping layers is opaque to users and does not provide a formal description of which layers can be skipped for a given input. Therefore, the

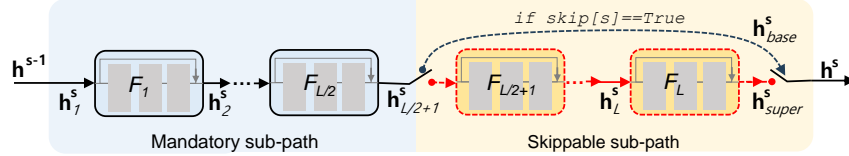


Figure 2: Illustration of a residual stage with two sub-paths. While the first (blue) sub-path is mandatory for hierarchical feature learning, the second (orange) sub-path can be skipped for efficiency. The layers in the skippable sub-path are trained to preserve the feature distribution from \mathbf{h}_{base}^s to \mathbf{h}_{super}^s using the proposed self-distillation strategy. Having similar feature distributions, either \mathbf{h}_{base}^s or \mathbf{h}_{super}^s can be provided as an input \mathbf{h}^s to the next residual stage. In the mandatory sub-path, another set of batch normalization operators, called *skip-aware BNs*, is exploited when the second sub-path is skipped. This architectural pattern is applicable to both CNNs and transformers.

network depths cannot be adapted in a predictable manner to meet the resource condition of target devices.

Residual Blocks with Shortcuts: Since the introduction of ResNets [34], residual blocks with identity shortcuts have received extensive attention because of their ability to train very deep networks, and have been chosen by many CNNs [35, 36] and transformers [1, 37, 38]. Veit et al. [39] argue that identity shortcuts make exponential paths and results in an ensemble of shallower sub-networks. This thought is supported by the fact that removing individual residual blocks at test time does not significantly affect performance, and it has been further exploited to train deep networks [40, 41]. Other works argue that identity shortcuts enable residual blocks to perform iterative feature refinement, where each block improves slightly but keeps the semantic of the representation of the previous layer [42, 43]. Our work build upon those views on residual blocks with shortcuts and further extend them for adaptive depth networks by introducing a training method that enforces the properties of residual blocks more explicitly for skippable sub-paths.

3 Adaptive Depth Networks

We first present the architecture and training details of adaptive depth networks. Then, we discuss the theoretic rationale for how depth adaptation can be achieved with minimal performance degradation.

3.1 Architectural Pattern for Depth Adaptation

In hierarchical networks, such as ResNets [34] and Swin transformers [38], there are typically 4 to 7 consecutive residual stages. In a network with N_r residual stages, the s -th ($s = 1, \dots, N_r$) residual stage consists of L identical residual blocks¹ that transform input features \mathbf{h}_1^s additively to produce the output features \mathbf{h}^s , as follows:

$$\underbrace{\mathbf{h}_1^s}_{=\mathbf{h}^{s-1}} + \underbrace{F_1(\mathbf{h}_1^s) + \dots + F_{L/2}^s(\mathbf{h}_{L/2}^s)}_{\mathbf{F}_{base}^s} + \underbrace{F_{L/2+1}^s(\mathbf{h}_{L/2+1}^s) \dots + F_L(\mathbf{h}_L^s)}_{\mathbf{F}_{skippable}^s} = \mathbf{h}^s \quad (1)$$

While a block with a residual function F_ℓ ($\ell = 1, \dots, L$) learns hierarchical features as traditional compositional networks [44], previous literature [43, 42] demonstrates that a residual function also tend to learn a function that refines already learned features at the same feature level. If a residual block mostly performs feature refinement while not changing the level of input features, the performance of the residual network is not significantly affected by dropping the block at test time [40, 41]. However, in typical residual networks, most residual blocks tend to refine features while learning new level features as well, and, hence, random dropping of residual blocks at test time degrades inference performance significantly. Therefore, we hypothesize that if some selected residual blocks can be encouraged explicitly during training to focus more on feature refinement, then these blocks can be skipped to save computation at marginal loss of prediction accuracy at test time.

To this end, we propose an architectural pattern for adaptive depth networks, in which every residual stage is divided into two sub-paths, or \mathbf{F}_{base}^s and $\mathbf{F}_{skippable}^s$ as in Equation 1 and Figure 2. We train

¹In transformers, residual blocks are called *encoder-decoder blocks*. In most networks, L is usually 3 to 6.

these two sub-paths to have different properties. While \mathbf{F}_{base}^s is trained to learn feature representation $\mathbf{h}_{base}^s (= \mathbf{h}_{L/2+1}^s)$ with no constraint, the second sub-path $\mathbf{F}_{skippable}^s$ is constrained to preserve the feature level of \mathbf{h}_{base}^s and only refine it to produce $\mathbf{h}_{super}^s (= \mathbf{h}_{L+1}^s)$. Since layers in \mathbf{F}_{base}^s perform essential transformations for hierarchical feature learning, they cannot be bypassed during inference. In contrast, layers in $\mathbf{F}_{skippable}^s$ can be skipped to save computation since they only refine \mathbf{h}_{base}^s . If $\mathbf{F}_{skippable}^s$ is skipped, then intermediate features \mathbf{h}_{base}^s becomes the input to the next residual stage. Therefore, 2^{N_r} sub-networks with different accuracy-efficiency trade-offs can be selected from a single network by choosing whether to skip $\mathbf{F}_{skippable}^s (s = 1, \dots, N_r)$ or not.

Table 4 in Appendix A.1 provides details on how this pattern is applied to both CNNs and transformers.

3.2 Training Sub-Paths with Self-Distillation

Preserving the feature level of \mathbf{h}_{base}^s in $\mathbf{F}_{skippable}^s$ implies, more specifically, that two feature representations \mathbf{h}_{base}^s and \mathbf{h}_{super}^s have similar distributions over training input \mathbf{X} . Algorithm 1 shows our training method, in which \mathbf{h}_{base}^s and \mathbf{h}_{super}^s are encouraged to have similar distributions by including *Kullback-Leibler* (KL) divergence between them, or $D_{KL}(\mathbf{h}_{super}^s || \mathbf{h}_{base}^s)$, in the loss function.

Algorithm 1 Training algorithm for an adaptive depth network \mathbf{M} . The forward function of \mathbf{M} accepts an extra argument, ‘skip’, which controls the residual stages where their skippable sub-paths are skipped. For example, the smallest sub-network, or *base-net*, of \mathbf{M} is selected by passing ‘skip=[True, True, True, True]’ when the total number of residual stages, denoted by N_r , is 4.

```

1: Initialize an adaptive depth network  $\mathbf{M}$ 
2: for  $i = 1$  to  $n_{iters}$  do
3:   Get next mini-batch of data  $\mathbf{x}$  and label  $\mathbf{y}$ 
4:    $optimizer.zero\_grad()$ 
5:    $\hat{\mathbf{y}}_{super}, \mathbf{h}_{super} = \mathbf{M}.forward(\mathbf{x}, skip=[False, \dots, False])$   $\triangleright$  forward pass for super-net
6:    $loss_{super} = criterion(\mathbf{y}, \hat{\mathbf{y}}_{super})$ 
7:    $loss_{super}.backward()$ 
8:    $\hat{\mathbf{y}}_{base}, \mathbf{h}_{base} = \mathbf{M}.forward(\mathbf{x}, skip=[True, \dots, True])$   $\triangleright$  forward pass for base-net
9:    $loss_{base} = \sum_{s=1}^{N_r} D_{KL}(\mathbf{h}_{super}^s || \mathbf{h}_{base}^s) + D_{KL}(\hat{\mathbf{y}}_{super} || \hat{\mathbf{y}}_{base})$ 
10:   $loss_{base}.backward()$   $\triangleright$  self-distillation of skippable sub-paths
11:   $optimizer.step()$ 
12: end for

```

In Algorithm 1, the largest and the smallest sub-networks of \mathbf{M} , which are called *super-net* and the *base-net*, respectively, are exploited. During the forward passes of the super-net and the base-net in steps 5 and 8, respectively, intermediate features \mathbf{h}_{super} and \mathbf{h}_{base} are obtained. In steps 9-10, $D_{KL}(\mathbf{h}_{super}^s || \mathbf{h}_{base}^s)$ in the loss function is explicitly minimized for training data \mathbf{X} . Further, this self-distillation step gives the effect of transferring the knowledge from \mathbf{h}_{super}^s to \mathbf{h}_{base}^s at every residual stage. Therefore, \mathbf{h}_{base}^s is expected to learn more compact representation from \mathbf{h}_{super}^s .

Self-distillation itself has been extensively used in prior adaptive networks [11, 10, 13]. However, their primary goal is to train every target sub-network. For example, on each iteration, sub-networks are randomly sampled from a large search space to act as either teachers or students [11], which results in significantly longer training time. In contrast, our method in Algorithm 1 focuses on training sub-paths by exclusively using the super-net as a teacher and the base-net as a student. By focusing on training sub-paths rather than target sub-networks, the training procedure in Algorithm 1 is significantly simplified. At test time, however, $2^{N_r} (= \sum_{k=0}^{N_r} C(N_r, k))$ different sub-networks can be constructed instantly by connecting these sub-paths in a combinatorial manner. The effect of this self-distillation strategy is investigated in Section 4.4.

3.3 Analysis of Skippable Sub-Paths

Formal Analysis: $D_{KL}(\mathbf{h}_{super}^s || \mathbf{h}_{base}^s)$ in the loss function $loss_{base}$ can be trivially minimized if residual blocks in $\mathbf{F}_{skippable}^s$ learn identity functions, or $\mathbf{h}_{base}^s + \mathbf{F}_{skippable}^s(\mathbf{h}_{base}^s) = \mathbf{h}_{base}^s$. However, since the super-net is jointly trained with the loss function $loss_{super}$, the residual functions in $\mathbf{F}_{skippable}^s$ cannot simply be an identity function. Then, what do the residual functions in $\mathbf{F}_{skippable}^s$

learn during training? This can be further investigated through Taylor expansion [43]. For our adaptive depth networks, a loss function \mathcal{L} used for training the super-net can be approximated with Taylor expansion as follows:

$$\mathcal{L}(\mathbf{h}_{super}^s) = \mathcal{L}\{\mathbf{h}_{base}^s + \mathbf{F}_{skippable}^s(\mathbf{h}_{base}^s)\} \quad (2)$$

$$= \mathcal{L}\{\mathbf{h}_{base}^s + F_{L/2+1}(\mathbf{h}_{L/2+1}^s) + \dots + F_{L-1}(\mathbf{h}_{L-1}^s) + F_L(\mathbf{h}_L^s)\} \quad (3)$$

$$\approx \mathcal{L}\{\mathbf{h}_{base}^s + F_{L/2+1}(\mathbf{h}_{L/2+1}^s) + \dots + F_{L-1}(\mathbf{h}_{L-1}^s)\} + F_L(\mathbf{h}_L^s) \cdot \frac{\partial \mathcal{L}(\mathbf{h}_L^s)}{\partial \mathbf{h}_L^s} + \mathcal{O}(F_L(\mathbf{h}_L^s)) \quad (4)$$

In Equation 4, the loss function is expanded around \mathbf{h}_L^s , or $\mathbf{h}_{base}^s + \dots + F_{L-1}(\mathbf{h}_{L-1}^s)$. Only the first order term is left and all high order terms, such as $F_L(\mathbf{h}_L^s)^2 \cdot \frac{\partial^2 \mathcal{L}(\mathbf{h}_L^s)}{2\partial(\mathbf{h}_L^s)^2}$, are absorbed in $\mathcal{O}(F_L(\mathbf{h}_L^s))$.

The high-order terms in $\mathcal{O}(F_L(\mathbf{h}_L^s))$ can be ignored if $F_L(\mathbf{h}_L^s)$ has a small magnitude. In typical residual networks, however, every layer is trained to learn new features with no constraint, and, hence, there is no guarantee that $F_L(\mathbf{h}_L^s)$ have small magnitude. In contrast, in our adaptive depth networks, the residuals in $\mathbf{F}_{skippable}^s$ are explicitly enforced to have small magnitude through the proposed self-distillation strategy, and, hence, the terms in $\mathcal{O}(F_L(\mathbf{h}_L^s))$ can be ignored for the approximation; see Figure 3 for empirical evidence. If we similarly keep expanding the loss function around \mathbf{h}_j^s ($j = L/2 + 1, \dots, L$) while ignoring high order terms, we obtain the following approximation:

$$\mathcal{L}(\mathbf{h}_{super}^s) \approx \mathcal{L}(\mathbf{h}_{base}^s) + \sum_{j=L/2+1}^L F_j(\mathbf{h}_j^s) \cdot \frac{\partial \mathcal{L}(\mathbf{h}_j^s)}{\partial \mathbf{h}_j^s} \quad (5)$$

In Equation 5, minimizing the loss $\mathcal{L}(\mathbf{h}_{super}^s)$ during training drives $F_j(\mathbf{h}_j^s)$ ($j = L/2 + 1, \dots, L$) in the negative half space of $\frac{\partial \mathcal{L}(\mathbf{h}_j^s)}{\partial \mathbf{h}_j^s}$ to minimize the dot product between $F_j(\mathbf{h}_j^s)$ and $\frac{\partial \mathcal{L}(\mathbf{h}_j^s)}{\partial \mathbf{h}_j^s}$. This implies that every residual function in $\mathbf{F}_{skippable}^s$ is optimized to learn a function that has a similar effect to gradient descent:

$$F_j(\mathbf{h}_j^s) \simeq - \frac{\partial \mathcal{L}(\mathbf{h}_j^s)}{\partial \mathbf{h}_j^s} \quad (j = L/2 + 1, \dots, L) \quad (6)$$

In other words, the residual functions in the skippable sub-paths reduce the loss $\mathcal{L}(\mathbf{h}_{base}^s)$ iteratively during inference while preserving the feature distribution of \mathbf{h}_{base}^s .

Considering this result, we can conjecture that, with our architectural pattern and self-distillation strategy, layers in $\mathbf{F}_{skippable}^s$ learn functions that refine input features \mathbf{h}_{base}^s iteratively for better inference accuracy while minimally changing the distribution of \mathbf{h}_{base}^s .

Empirical Analysis: We can estimate how much the distribution of input \mathbf{h} is transformed by residual function F by measuring $\|F(\mathbf{h})\|_2 / \|\mathbf{h}\|_2$ at each residual block. Figure 3 illustrates $\|F(\mathbf{h})\|_2 / \|\mathbf{h}\|_2$ at every residual block in the baseline ResNet50 and our ResNet50-ADN that is trained according to Algorithm 1². Our ResNet50-ADN exhibits greater transformation than ResNet50 in the mandatory sub-paths (blue areas) and less transformation in the skippable sub-paths (orange areas). This result demonstrates that our self-distillation strategy in Algorithm 1 effectively trains the skippable sub-paths to minimally change the input distribution. As a result, the blocks in skippable sub-paths can be skipped with less impact on performance.

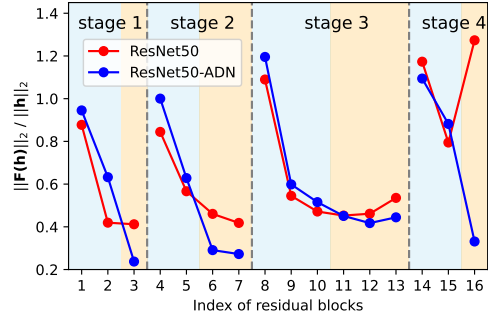


Figure 3: $\|F(\mathbf{h})\|_2 / \|\mathbf{h}\|_2$ at residual blocks. In ours, skippable sub-paths (orange areas) minimally change the distribution of input \mathbf{h}

3.4 Skip-Aware Batch/Layer Normalization

Originally, batch normalization (BN) [45] was proposed to handle internal covariate shift during training non-adaptive networks by normalizing features. In our adaptive depth networks, however,

²ImageNet validation dataset is used for this experiment.

internal covariate shifts can occur during inference in mandatory sub-paths if different sub-networks are selected. To handle potential internal covariate shifts, switchable BN operators, called *skip-aware BNs*, are used in mandatory sub-paths. For example, at each residual stage, two sets of BNs are available for the mandatory sub-path, and they are switched depending on whether its skippable sub-path is skipped or not.

The effectiveness of switchable BNs has been demonstrated in networks with adaptive widths [46, 11] and adaptive resolutions [47]. However, in previous adaptive networks, N sets of switchable BNs are required in every layer to support N parameter-sharing sub-networks. Such a large number of switchable BNs not only requires more parameters, but also makes the training process complicated since N sets of switchable BNs need to be trained iteratively during training. In contrast, in our adaptive depth networks, every mandatory sub-path needs only two sets of switchable BNs, regardless of the number of supported sub-networks. This reduced number of switchable BNs significantly simplifies the training process as shown in Algorithm 1. Furthermore, the amount of parameters for skip-aware BNs is negligible. For instance, in ResNet50, skip-aware BNs increase the parameters by 0.07%.

Transformers [1, 38] exploit layer normalization (LN) instead of BNs and naive replacement of LNs to BNs incurs instability during training [48]. Therefore, for our adaptive depth transformers, we apply switchable LN operators in mandatory sub-paths instead of switchable BNs.

4 Experiments

We use four representative residual networks both from CNNs and vision transformers as base models to apply the proposed architecture pattern: MobileNet V2 [35] is a lightweight CNN model, ResNet [34] is a larger CNN model, and ViT [37] and Swin-T [38] are representative vision transformers. All base models except ViT have hierarchical stages, each with 2 \sim 6 residual blocks. So, according to the proposed architectural pattern, every residual stage is evenly divided into 2 sub-paths for depth adaptation. ViT does not define hierarchical stages and all residual encoder blocks have same spatial dimensions. Therefore, we divide 12 encoder blocks into 4 groups, resembling other residual networks, and select the last encoder block of each group as a skippable sub-path. Details are in Table 4 in Appendix A.1.

We use the suffix ‘-ADN’ to denote our adaptive depth networks. Since our adaptive depth networks have many parameter-sharing sub-networks in a single network, we indicate which sub-network is used for evaluation in parenthesis, e.g., ResNet50-ADN (super-net). For our sub-networks, boolean values are also used to indicate in which residual stages the sub-paths are skipped. For example, ResNet50-ADN (base-net) is equivalent to ResNet50-ADN (TTTT).

4.1 ImageNet Classification

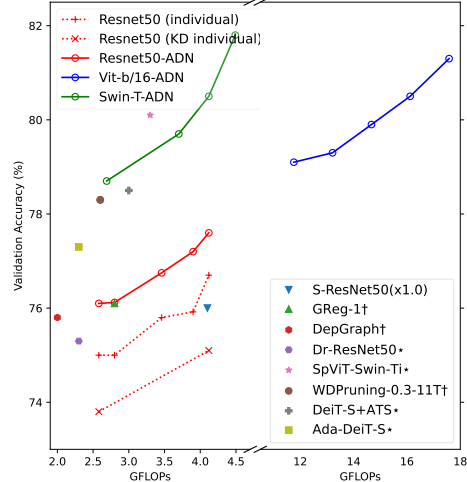
We evaluate our method on ILSVRC2012 dataset [49] that has 1000 classes. The dataset consists of 1.28M training and 50K validation images. For CNN models, we follow most training settings in the original papers [34, 35], except that ResNet models are trained for 150 epochs. ViT and Swin-T are trained for 300 epochs, following DeiT’s training recipe [50, 51]. For Swin-T-ADN, we disable stochastic depths [40] for the mandatory sub-paths since the strategy of random dropping of residual blocks conflicts with our approach to skipping sub-paths. For fair comparison, our adaptive depth networks and corresponding individual networks are trained in the same training settings.

The results in Figure 4-(a) show that our adaptive depth networks outperform counterpart individual networks even though many sub-networks share parameters in a single model. Further, our results with vision transformers demonstrate that our approach is generally applicable and compatible with their state-of-the-art training techniques such as DeiT’s training recipe [50]. We conjecture that this performance improvement results from effective distillation of knowledge from \mathbf{h}_{super}^s to \mathbf{h}_{base}^s at each residual stage and the iterative feature refinement at skippable sub-paths, shown in Equation 6.

Figure 4-(b) shows Pareto frontiers formed by selected sub-networks of our adaptive depth networks; Table 5 in Appendix A.2 shows the performance of all sub-networks. In Figure 4-(b) and Table 1, several state-of-the-art efficient inference methods and dynamic networks are compared with our base-networks. The result demonstrates that our adaptive depth networks show competitive performance across a range of FLOPs. In Figure 4-(b), it should be noted that individual ResNets

Model	Params (M)	FLOPs (G)	Acc (%)
ResNet50-ADN (FFFF)	25.58	4.11	77.6
ResNet50-ADN (TTTT)		2.58	76.1
ResNet50	25.56	4.11	76.7
ResNet50-Base	17.11	2.58	75.0
MbV2-ADN (FFFF)	3.72	0.32	72.7
MbV2-ADN (TTTT)		0.25	70.7
MbV2	3.50	0.32	72.1
MbV2-Base	2.99	0.25	70.7
ViT-b/16-ADN (FFFF)	86.59	17.58	81.3
ViT-b/16-ADN (TTTT)		11.76	79.4
ViT-b/16	86.57	17.58	81.1
ViT-b/16-Base	67.70	11.76	78.7
Swin-T-ADN (FFFF)	28.30	4.49	81.8
Swin-T-ADN (TTTT)		2.69	78.7
Swin-T	28.29	4.49	81.5
Swin-T-Base	15.63	2.69	78.6

(a) Results on ImageNet



(b) Pareto frontiers of our networks

Figure 4: (a) Results on ImageNet validation dataset. Networks with the suffix ‘-Base’ have the same depths as the base-nets of corresponding adaptive depth networks. (b) Pareto frontiers formed by the sub-networks of our adaptive depth networks. ResNet50 (individual) and ResNet50 (KD individual) are non-adaptive networks having same depths as the sub-networks of ResNet50-ADN.

Table 1: Our base-nets are compared with state-of-the-art efficient inference methods. † denotes static pruning methods, * denotes width-adaptation networks, and * denotes input-dependent dynamic pruning. While these approaches exploit various non-canonical training techniques, such as iterative retraining, our base-nets are instantly selected from adaptive depth networks without fine-tuning.

Model	FLOPs	↓FLOPs	Acc@1
GReg-1 [55]†	2.8G	33%	76.1%
DepGraph [56]†	2.0G	51%	75.8%
DR-ResNet50 ($\alpha=2.0$) [47]*	2.3G	44%	75.3%
ResNet50-ADN (TTTT)	2.6G	37%	76.1%
AlphaNet-0.75x [11] *	0.21G	34%	70.5%
MbV2-ADN (TTTT)	0.25G	22%	70.7%
WDPruning-0.3-11 [57]†	2.6G	-	78.3%
X-Pruner [58] †	3.2G	28%	80.7%
Ada-DeiT-S [27]*	2.3G	-	77.3%
SPViT-Swin-Ti [59]*	3.3G	27%	80.1%
Swin-T-ADN (TTTT)	2.7G	40%	78.7%

trained with knowledge distillation has worse performance than individual ResNets. As reported in previous works, successful knowledge distillation requires a patient and long training [52], and straightforward knowledge distillation using ImageNet does not improve the performance of student models [53, 54]. In contrast, our ResNet50-ADN trained with the proposed self-distillation strategy achieves better performance than counterpart ResNets. This demonstrates that the high performance of adaptive depth networks does not simply come from distillation effect.

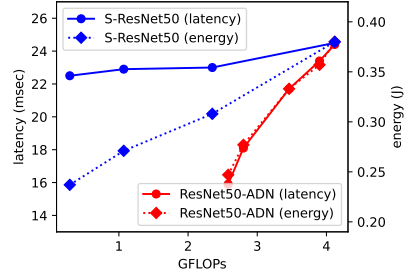
4.2 Training Time

One major advantage of our adaptive depth networks is that they require significantly shorter training time than prior adaptive networks. Figure 5-(a) shows that training our adaptive depth networks take similar time to train two individual networks combined. This is because our training method in Algorithm 1 exclusively exploits only the super-net and the base-net for self-distillation. In contrast, compared adaptive networks require much longer training time than ours since they have to train every target sub-network explicitly³. For example, on every training iteration, AlphaNet [11] randomly

³Although the prior works we compared for training time may seem outdated, they remain relevant and representative because there has been little progress in reducing the training time of adaptive networks.

Model	1 epoch (min)	# of sub-nets
ResNet50	32.9	-
ResNet50-Base	22.7	-
ResNet50-ADN (ours)	54.7	2 ⁴ depths
MSDNet [8]	67.1	9 depths
S-ResNet50 [10]	82.5	4 widths
MbV2	13.1	-
MbV2-Base	10.0	-
MbV2-ADN (ours)	22.5	2 ⁴ depths
AlphaNet* [11]	230.5	216 depths

(a) Training time



(b) On-device Inference latency/energy

Figure 5: (a) Training time (1 epoch), measured on Nvidia RTX 4090 (batch size: 128). AlphaNet* is configured to have similar FLOPs to MbV2 and makes sub-networks by only adjusting the network depth. (b) Inference latency and energy consumption of adaptive networks, measured on Nvidia Jetson Orin Nano (batch size: 1)

samples sub-networks from its search space for self-distillation. While AlphaNet [11] supports significantly more sub-networks, it should be noted that supporting many sub-networks is not our goal. Instead, our objective is to provide better performance Pareto with several useful sub-networks, as demonstrated in Figure 4-(b). For example, although ResNet50-ADN can select 2⁴ sub-networks, Table 5 (in Appendix A.2) shows that some sub-networks are more useful than the others; results in Table 5 show that skipping sub-paths in deeper residual stages is more detrimental to the performance in general, implying that refinement of features is more needed for deeper residual stages.

4.3 On-Device Performance

While the Pareto frontiers formed by sub-networks demonstrate theoretic performance, inference acceleration in actual devices is more important in practice for effective control of inference latency and energy consumption.

Figure 5b shows the performance in Nvidia Jetson Orin Nano. The inference latency and energy consumption of ResNet50-ADN is compared to S-ResNet50, a representative width-adaptation network. The result shows that depth-adaptation of ResNet50-ADN is highly effective in accelerating inference speeds and reducing energy consumption. For example, in ResNet50-ADN, reducing FLOPs by 38% through depth adaptation reduces both inference latency and energy consumption by 35%. In contrast, even though S-ResNet50 can reduce FLOPs by up to 93% by adjusting its width, it only achieves up to 9% acceleration in practice.

4.4 Ablation Study

Table 2: Ablation analysis with ResNet50-ADN and ViT-b/32-ADN. Applied components are checked. ↓ and ↑ in parentheses are comparisons to non-adaptive individual networks.

self-distillation.	skip-aware BNs/LNs	ResNet50 Acc@1 (%)		ViT-b/32 Acc@1 (%)	
		FFFF	TTTT	FFFF	TTTT
		75.2% (↓ 1.5%)	72.2% (↓ 2.8%)	75.7% (↓ 0.2%)	74.1% (↑ 0.3%)
O		76.1% (↓ 0.6%)	74.9% (↓ 0.1%)	76.4% (↑ 0.5%)	74.3% (↑ 0.5%)
	O	76.6% (↓ 0.1%)	75.1% (↑ 0.1%)	76.0% (↑ 0.1%)	74.3% (↑ 0.5%)
O	O	77.6% (↑ 0.9%)	76.1% (↑ 1.1%)	76.6% (↑ 0.8%)	74.3% (↑ 0.5%)

We first investigate the influence of two key components of the proposed adaptive depth networks: (1) self-distillation of sub-paths and (2) skip-aware BNs/LNs. When our self-distillation method is not applied, the loss of the base-net, or $loss_{base}$, in Algorithm 1 is modified to $criterion(\mathbf{y}, \hat{\mathbf{y}}_{base})$. Table 2 shows the results. For ResNet50, when neither of them is applied, the inference accuracy of the super-net and the base-net is significantly lower than non-adaptive individual networks by 1.5% and 2.8%, respectively. This result shows the difficulty of joint training sub-networks for adaptive networks. When one of the two components is applied individually, the performance is still

slightly worse than individual networks’. In the last row, when both self-distillation and skip-aware BNs are applied together, ResNet50-ADN achieves significantly better performance than individual networks, both in the super-net and the base-net. The results with ViT-b/32 show that switchable layer normalization has similar effect in vision transformers.

Table 3: Comparison of self-distillation strategies. Our approach (in bold) uses exclusively the super-net and the base-net as a teacher and a student, respectively.

sub-nets		ResNet50-ADN Acc@1 (%)					ViT/b-32-ADN Acc@1 (%)				
Teacher	Student	FFFF	TFFF	TTFF	TTTF	TTTT	FFFF	TFFF	TTFF	TTTF	TTTT
FFFF	TTTT	77.6	77.2	76.8	76.1	76.1	76.6	76.0	75.5	74.5	74.3
FFFF	Random	77.1	76.7	76.4	75.5	74.8	75.2	74.7	73.9	72.9	71.1
Random	TTTT	75.5	75.5	75.4	75.0	74.9	72.0	72.0	71.9	71.8	71.7
Random	Random	75.4	75.2	75.2	74.9	74.6	70.8	70.7	70.6	70.4	70.3

Self-Distillation Strategies: Our self-distillation approach in Algorithm 1 exploits only two sub-networks exclusively as a teacher and a student. Specifically, the super-nets, or FFFF, acts as the teacher and the base-nets, or TTTT, becomes the student. The purpose of this strategy is not to train only those two sub-networks, but rather to train skippable sub-paths in a way that minimally modifies the feature distribution, as demonstrated in Figure 3. To investigate the effect of self-distillation strategies, we conduct an experiment in Table 3. In every training iteration, rather than exclusively using FFFF and TTTT sub-networks for self-distillation, we randomly sample either a teacher, a student, or both from 2^4 sub-networks. These randomly sampled sub-networks are trained explicitly through self-distillation. However, as shown in Table 3, all sub-networks, both from ResNet50-ADN and ViT/b-32-ADN, perform significantly better when our self-distillation strategy is applied for training. Even though some sub-networks (such as TTTF, TTFF, and TFFF) are not trained explicitly with our self-distillation strategy, they still outperform their counterpart sub-networks trained through random sampling. This result demonstrates that our method of training sub-paths is more effective than training target sub-networks themselves.

Lengths of Mandatory Sub-Paths: In Figure 6, we investigate the effect of varying the length ratio between the mandatory and the skippable sub-paths. (Details are in Table 6.) If mandatory sub-paths become shorter than skippable sub-paths, smaller sub-networks can be selected since more layers can be skipped. However, the result in Figure 6 shows that this configuration significantly degrades performance of all sub-networks. Since every sub-network shares parameters of mandatory sub-paths, low inference capability of shallow mandatory sub-paths affects all sub-networks. This implies that maintaining certain depths in mandatory sub-paths is essential for effective inference. In contrast, increasing the length of mandatory sub-paths further does not yield further performance improvement and only reduce the range of FLOPs adaptation.

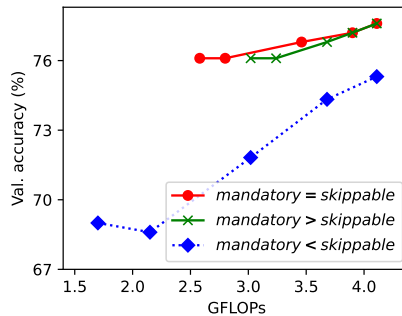


Figure 6: Pareto frontiers of ResNet50-ADNs trained with varying ratios between mandatory and skippable sub-paths. Total number of blocks remains unchanged.

5 Conclusions

We propose a practical approach to adaptive depth networks that can be applied to both CNNs and transformers with minimal training effort. We provide a general principle and formal explanation on how depth adaptation can be achieved with minimal performance degradation. Under this principle, our approach can avoid typical exhaustive training of target sub-network and instead focus on optimizing the sub-paths of the network to have specific properties. At test time, those sub-paths can be connected in a combinatorial manner to construct sub-networks with various accuracy-efficiency trade-offs from a single network. Experimental results show that those sub-networks form a better Pareto frontier than non-adaptive baseline networks and achieve actual inference acceleration.

References

- [1] Vaswani, A., N. Shazeer, N. Parmar, et al. Attention is all you need. In *Conference on Neural Information Processing Systems (NeurIPS)*, vol. 30. 2017.
- [2] Howard, A. G., M. Zhu, B. Chen, et al. Mobilenets: Efficient convolutional neural networks for mobile vision applications. *arXiv preprint arXiv:1704.04861*, 2017.
- [3] Han, K., Y. Wang, Q. Tian, et al. Ghostnet: More features from cheap operations. In *IEEE/CVF Conference on Computer Vision and Pattern Recognition (CVPR)*. 2020.
- [4] Han, S., H. Mao, W. J. Dally. Deep compression: Compressing deep neural network with pruning, trained quantization and huffman coding. In *International Conference on Learning Representations (ICLR)*. 2016.
- [5] Liu, Z., H. Mu, X. Zhang, et al. Metapruning: Meta learning for automatic neural network channel pruning. In *International Conference on Computer Vision (ICCV)*, pages 3296–3305. 2019.
- [6] Jacob, B., S. Kligys, B. Chen, et al. Quantization and training of neural networks for efficient integer-arithmetic-only inference. In *Conference on Computer Vision and Pattern Recognition (CVPR)*. 2018.
- [7] Hinton, G., O. Vinyals, J. Dean. Distilling the knowledge in a neural network. *arXiv preprint arXiv:1503.02531*, 2015.
- [8] Huang, G., D. Chen, T. Li, et al. Multi-scale dense networks for resource efficient image classification. In *International Conference on Learning Representations (ICLR)*. 2018.
- [9] Fan, A., E. Grave, A. Joulin. Reducing transformer depth on demand with structured dropout. In *International Conference on Learning Representations (ICLR)*. 2020.
- [10] Yu, J., L. Yang, N. Xu, et al. Slimmable neural networks. In *International Conference on Learning Representations (ICLR)*. 2019.
- [11] Wang, D., C. Gong, M. Li, et al. Alphanet: Improved training of supernet with alpha-divergence. In M. Meila, T. Zhang, eds., *International Conference on Machine Learning (ICML)*, vol. 139 of *Proceedings of Machine Learning Research*, pages 10760–10771. PMLR, 2021.
- [12] Wan, C., H. Hoffmann, S. Lu, et al. Orthogonalized sgd and nested architectures for anytime neural networks. In *International Conference on Machine Learning (ICML)*, pages 9807–9817. PMLR, 2020.
- [13] Hou, L., Z. Huang, L. Shang, et al. Dynabert: Dynamic bert with adaptive width and depth. *Conference on Neural Information Processing Systems (NeurIPS)*, 33, 2020.
- [14] Touvron, H., M. Cord, M. Oquab, et al. Co-training 2l submodels for visual recognition. In *Conference on Computer Vision and Pattern Recognition (CVPR)*. 2023.
- [15] Li, H., H. Zhang, X. Qi, et al. Improved techniques for training adaptive deep networks. In *International Conference on Computer Vision (ICCV)*, pages 1891–1900. 2019.
- [16] Gong, C., D. Wang, M. Li, et al. NASVit: Neural architecture search for efficient vision transformers with gradient conflict aware supernet training. In *International Conference on Learning Representations (ICLR)*. 2022.
- [17] Hu, H., D. Dey, M. Hebert, et al. Learning anytime predictions in neural networks via adaptive loss balancing. In *Proceedings of the AAAI Conference on Artificial Intelligence*, vol. 33, pages 3812–3821. 2019.
- [18] Zhang, L., J. Song, A. Gao, et al. Be your own teacher: Improve the performance of convolutional neural networks via self distillation. In *International Conference on Computer Vision (ICCV)*, pages 3713–3722. 2019.
- [19] Beyer, L., P. Izmailov, A. Kolesnikov, et al. Flexivit: One model for all patch sizes. In *Conference on Computer Vision and Pattern Recognition (CVPR)*. 2023.
- [20] Yu, J., T. S. Huang. Universally slimmable networks and improved training techniques. In *International Conference on Computer Vision (ICCV)*, pages 1803–1811. 2019.
- [21] Han, Y., G. Huang, S. Song, et al. Dynamic neural networks: A survey. *IEEE Transactions on Pattern Analysis and Machine Intelligence*, 44(11):7436–7456, 2022.

- [22] Wu, Z., T. Nagarajan, A. Kumar, et al. Blockdrop: Dynamic inference paths in residual networks. In *Conference on Computer Vision and Pattern Recognition (CVPR)*, pages 8817–8826. 2018.
- [23] Li, C., G. Wang, B. Wang, et al. Dynamic slimmable network. In *Conference on Computer Vision and Pattern Recognition (CVPR)*, pages 8607–8617. 2021.
- [24] Guo, Q., Z. Yu, Y. Wu, et al. Dynamic recursive neural network. In *2019 IEEE/CVF Conference on Computer Vision and Pattern Recognition (CVPR)*, pages 5142–5151. 2019.
- [25] Li, Y., L. Song, Y. Chen, et al. Learning dynamic routing for semantic segmentation. In *Conference on Computer Vision and Pattern Recognition (CVPR)*. 2020.
- [26] Yang, L., Y. Han, X. Chen, et al. Resolution adaptive networks for efficient inference. In *Proceedings of the IEEE Conference on Computer Vision and Pattern Recognition*. 2020.
- [27] Meng, L., H. Li, B. Chen, et al. Adavit: Adaptive vision transformers for efficient image recognition. In *Conference on Computer Vision and Pattern Recognition (CVPR)*, pages 12299–12308. 2022.
- [28] Yin, H., A. Vahdat, J. M. Alvarez, et al. A-ViT: Adaptive tokens for efficient vision transformer. In *Conference on Computer Vision and Pattern Recognition (CVPR)*, pages 10809–10818. 2022.
- [29] Fayyaz, M., S. A. Koohpayegani, F. R. Jafari, et al. Adaptive token sampling for efficient vision transformers. In S. Avidan, G. Brostow, M. Cissé, G. M. Farinella, T. Hassner, eds., *European Conference on Computer Vision (ECCV)*, pages 396–414. 2022.
- [30] Heo, B., S. Yun, D. Han, et al. Rethinking spatial dimensions of vision transformers. In *International Conference on Computer Vision (ICCV)*. 2021.
- [31] Figurnov, M., M. D. Collins, Y. Zhu, et al. Spatially adaptive computation time for residual networks. In *Conference on Computer Vision and Pattern Recognition (CVPR)*, pages 1039–1048. 2017.
- [32] Veit, A., S. Belongie. Convolutional networks with adaptive inference graphs. In *European Conference on Computer Vision (ECCV)*, pages 3–18. 2018.
- [33] Wang, X., F. Yu, Z.-Y. Dou, et al. Skipnet: Learning dynamic routing in convolutional networks. In *European Conference on Computer Vision (ECCV)*, pages 409–424. 2018.
- [34] He, K., X. Zhang, S. Ren, et al. Deep residual learning for image recognition. In *Conference on Computer Vision and Pattern Recognition (CVPR)*, pages 770–778. 2016.
- [35] Sandler, M., A. Howard, M. Zhu, et al. Mobilenetv2: Inverted residuals and linear bottlenecks. In *Conference on Computer Vision and Pattern Recognition (CVPR)*, pages 4510–4520. 2018.
- [36] Tan, M., Q. Le. Efficientnet: Rethinking model scaling for convolutional neural networks. In *International Conference on Machine Learning (ICML)*, pages 6105–6114. PMLR, 2019.
- [37] Dosovitskiy, A., L. Beyer, A. Kolesnikov, et al. An image is worth 16x16 words: Transformers for image recognition at scale. In *International Conference on Learning Representations (ICLR)*. 2021.
- [38] Liu, Z., Y. Lin, Y. Cao, et al. Swin transformer: Hierarchical vision transformer using shifted windows. In *International Conference on Computer Vision (ICCV)*. 2021.
- [39] Veit, A., M. J. Wilber, S. Belongie. Residual networks behave like ensembles of relatively shallow networks. *Conference on Neural Information Processing Systems (NeurIPS)*, 29:550–558, 2016.
- [40] Huang, G., Y. Sun, Z. Liu, et al. Deep networks with stochastic depth. In *European Conference on Computer Vision (ECCV)*, pages 646–661. Springer, 2016.
- [41] Xie, Q., M.-T. Luong, E. Hovy, et al. Self-training with noisy student improves imagenet classification. In *Conference on Computer Vision and Pattern Recognition (CVPR)*, pages 10687–10698. 2020.
- [42] Greff, K., R. K. Srivastava, J. Schmidhuber. Highway and residual networks learn unrolled iterative estimation. In *International Conference on Learning Representations (ICLR)*. 2016.
- [43] Jastrzebski, S., D. Arpit, N. Ballas, et al. Residual connections encourage iterative inference. In *International Conference on Learning Representations (ICLR)*. 2018.
- [44] Simonyan, K., A. Zisserman. Very deep convolutional networks for large-scale image recognition. In *3th International Conference on Learning Representations (ICLR)*. 2015.

- [45] Ioffe, S., C. Szegedy. Batch normalization: Accelerating deep network training by reducing internal covariate shift. In *International Conference on Machine Learning (ICML)*, pages 448–456. PMLR, 2015.
- [46] Yu, J., T. Huang. Autoslim: Towards one-shot architecture search for channel numbers. *arXiv preprint*, 2019.
- [47] Zhu, M., K. Han, E. Wu, et al. Dynamic resolution network. In *Conference on Neural Information Processing Systems (NeurIPS)*, vol. 35, pages 10985–10998. 2021.
- [48] Yao, Z., Y. Cao, Y. Lin, et al. Leveraging batch normalization for vision transformers. In *2021 IEEE/CVF International Conference on Computer Vision Workshops (ICCVW)*, pages 413–422. 2021.
- [49] Russakovsky, O., J. Deng, H. Su, et al. Imagenet large scale visual recognition challenge. *International journal of computer vision*, 115(3):211–252, 2015.
- [50] Touvron, H., M. Cord, M. Douze, et al. Training data-efficient image transformers & distillation through attention. *arXiv preprint*, 2020.
- [51] PyTorch. Image classification reference training scripts in pytorch, 2023.
- [52] Beyer, L., X. Zhai, A. Royer, et al. Knowledge distillation: A good teacher is patient and consistent. In *Conference on Computer Vision and Pattern Recognition (CVPR)*, pages 10925–10934. 2022.
- [53] Zagoruyko, S., N. Komodakis. Paying more attention to attention: Improving the performance of convolutional neural networks via attention transfer. In *5th International Conference on Learning Representations, ICLR*,. 2017.
- [54] Cho, J. H., B. Hariharan. On the efficacy of knowledge distillation. In *International Conference on Computer Vision (ICCV)*, pages 4794–4802. 2019.
- [55] Wang, H., C. Qin, Y. Zhang, et al. Neural pruning via growing regularization. In *International Conference on Learning Representations (ICLR)*. 2021.
- [56] Fang, G., X. Ma, M. Song, et al. Depgraph: Towards any structural pruning. In *Conference on Computer Vision and Pattern Recognition (CVPR)*, pages 16091–16101. 2023.
- [57] Yu, F., K. Huang, M. Wang, et al. Width & depth pruning for vision transformers. *Proceedings of the AAAI Conference on Artificial Intelligence*, 36(3):3143–3151, 2022.
- [58] Yu, L., W. Xiang. X-pruner: explainable pruning for vision transformers. In *Proceedings of the IEEE/CVF Conference on Computer Vision and Pattern Recognition (CVPR)*, pages 24355–24363. 2023.
- [59] Kong, Z., P. Dong, X. Ma, et al. Spvit: Enabling faster vision transformers via latency-aware soft token pruning. In S. Avidan, G. Brostow, M. Cissé, G. M. Farinella, T. Hassner, eds., *European Conference on Computer Vision (ECCV)*, pages 620–640. 2022.
- [60] Ren, S., K. He, R. Girshick, et al. Faster r-cnn: Towards real-time object detection with region proposal networks. *IEEE Transactions on Pattern Analysis and Machine Intelligence*, 2017.
- [61] He, K., G. Gkioxari, P. Dollár, et al. Mask r-cnn. In *International Conference on Computer Vision (ICCV)*, pages 2961–2969. 2017.
- [62] Lin, T.-Y., P. Dollár, R. Girshick, et al. Feature pyramid networks for object detection. In *Conference on Computer Vision and Pattern Recognition (CVPR)*. 2017.
- [63] Selvaraju, R. R., M. Cogswell, A. Das, et al. Grad-cam: Visual explanations from deep networks via gradient-based localization. In *International Conference on Computer Vision (ICCV)*, pages 618–626. 2017.

A Appendix: Detailed Settings and Evaluation Results

A.1 Detailed Architectures

	number of mandatory blocks	number of skippable blocks	total blocks
stage 1	2	1	3
stage 2	2	2	4
stage 3	3	3	6
stage 4	2	1	3

(a) ResNet50-ADN

	number of mandatory blocks	number of skippable blocks	total blocks
stage 1	2	1	3
stage 2	2	1	3
stage 3	2	1	3
stage 4	2	1	3

(b) ViT-b/16-ADN

	number of mandatory blocks	number of skippable blocks	total blocks
stage 1	1	-	1
stage 2	2	-	2
stage 3	2	1	3
stage 4	2	2	4
stage 5	2	1	3
stage 6	2	1	3
stage 7	1	-	1

(c) MbV2-ADN

	number of mandatory blocks	number of skippable blocks	total blocks
stage 1	1	1	2
stage 2	1	1	2
stage 3	3	3	6
stage 4	2	-	2

(d) Swin-T-ADN

Table 4: Each residual stage of base models is evenly divided into two sub-paths; the first is mandatory and the other is skippable. Since ViT does not define hierarchical stages, 12 identical encoder blocks are divided into 4 stages, resembling other residual networks for vision tasks.

A.2 Performance of Sub-Networks

sub-network	FLOPs (G)	Acc@1 (%)
FFFF	4.11	77.6
TFFF	3.90	77.2
FTFF	3.68	76.5
FFTF	3.46	75.6
FFFT	3.90	76.2
TTFE	3.46	76.8
TFTE	3.24	75.4
TFET	3.68	76.1
FTTE	3.02	75.3
FTET	3.46	75.4
FFTE	3.25	75.6
TTTE	2.80	76.1
TTET	3.24	75.9
TFET	3.02	75.4
FTTE	2.80	75.6
TTTT	2.58	76.1

(a) ResNet50-ADN

sub-network	FLOPs (G)	Acc@1 (%)
FFFF	17.58	81.3
TFFF	16.20	80.5
FTFF	16.20	80.2
FFTF	16.20	80.0
FFFT	16.20	80.4
TTFE	14.67	79.9
TFTE	14.67	79.6
TFET	14.67	79.8
FTTE	14.67	79.4
FTET	14.67	79.7
FFTE	14.67	79.4
TTTE	13.21	79.3
TTET	13.21	79.4
TFET	13.21	79.2
FTTE	13.21	79.1
TTTT	11.76	79.1

(b) ViT-b/16-ADN

Table 5: FLOPs and ImageNet validation accuracy of sub-networks. Only the super-net and the base-net are trained explicitly. The other parameter-sharing sub-networks in the middle can be selected at test time without explicit training. The highest accuracy in each group is shown in bold. This results show that skipping sub-paths in deeper residual stages is more detrimental to the performance in general, implying that refinement of features is more needed for deeper residual stages.

A.3 Varying the Lengths of Sub-Paths in ResNet50-ADN

	number of mandatory blocks	number of skippable blocks	total blocks
stage 1	1	2	3
stage 2	1	3	4
stage 3	2	4	6
stage 4	1	2	3

(a) # of mandatory < # of skippable

	number of mandatory blocks	number of skippable blocks	total blocks
stage 1	2	1	3
stage 2	3	1	4
stage 3	4	2	6
stage 4	2	1	3

(b) # of mandatory > # of skippable

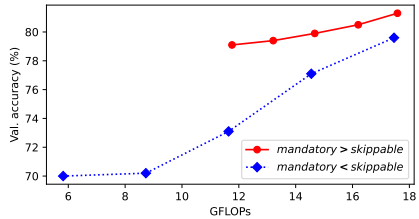
Table 6: Varying the length ratio of sub-paths of ResNet50-ADN. Total number of blocks of each stage is not changed.

A.4 Varying Sub-Paths Length Ratios in Vit-b/16-ADN

Each stage of Vit-b/16-ADN has 3 encoder blocks and, by default, we select every last encoder block as a skippable sub-path. Therefore every stage has two mandatory blocks and 1 skipable blocks as shown in Table 4-(b). Figure 7-(a) shows different configuration where every last two blocks of the stages become skippable. With this configuration in Figure 7-(a), we can select much smaller sub-networks. For example, the smallest sub-network, or the base-net, of Vit-b/15-ADN has only 4 mandatory blocks and it requires 5.82 GFLOPs. However, the result in Figure 7-(b) shows that this configuration significantly degrades performance of all sub-networks. As demonstrated with ResNet50-ADN in Figure 6, low inference capability of shallow mandatory sub-paths affects all sub-networks. This again shows that some minimum depths in mandatory sub-paths is required for effective inference.

	number of mandatory blocks	number of skippable blocks	total blocks
stage 1	1	2	3
stage 2	1	2	3
stage 3	1	2	3
stage 4	1	2	3

(a) # of mandatory < # of skippable



(b) Pareto frontiers of Vit-b/16-ADN

Figure 7: (a) The configuration of Vit-b/16-ADN with longer skippable sub-paths. (b) Pareto-frontier when different length ratios between the mandatory and the skippable sub-paths are applied.

B Appendix: More Experiments and Analysis

B.1 Object Detection and Instance Segmentation

Table 7: Object detection and instance segmentation results on MS COCO dataset.

Detector	Backbone	FLOPs	Individual Networks		ResNet50-ADN (ours)	
			Box AP	Mask AP	Box AP	Mask AP
Faster-RCNN	ResNet50	207.07G	36.4		37.8	
[60]	ResNet50-Base	175.66G	32.4		34.0	
Mask-RCNN	ResNet50	260.14G	37.2	34.1	38.3	34.1
[61]	ResNet50-Base	228.73G	32.7	29.9	34.1	31.2

In order to investigate the generalization ability of our approach, we use MS COCO 2017 datasets on object detection and instance segmentation tasks using representative detectors. We compare individual ResNet50 and our adaptive depth ResNet50-ADN as backbone networks of the detectors.

For training of detectors, we use Algorithm 1 with slight adaptation. For object detection, the intermediate features \mathbf{h}_{base}^s and \mathbf{h}_{super}^s ($s = 1..N_r$) can be obtained directly from backbone network’s feature pyramid networks (FPN) [62], and, hence, a wrapper function is not required to extract intermediate features. All networks are trained on train2017 for 12 epochs from ImageNet pretrained weights, following the training settings suggested in [62]. Table 7 shows the results on val2017 containing 5000 images. Our adaptive depth backbone networks still outperform individual static backbone networks in terms of COCO’s standard metric AP.

B.2 Visual Analysis of Sub-Paths

To investigate how our training method affects feature representations in the mandatory and the skippable sub-paths, we visualize the activation of 3rd residual stage of ResNet50-ADN using Grad-CAM [63]. The 3rd residual stage of ResNet50-ADN has 6 residual blocks and the last three blocks are skippable. In Figure 8-(a), the activation regions of original ResNet50 changes gradually across all consecutive blocks. In contrast, in Figure 8-(b), ResNet50-ADN(FFFF), or super-net, manifests very different activation regions in two sub-paths. In the first three residual blocks, we can observe lots of hot activation regions in wide areas, suggesting active learning of new level features. In contrast, significantly less activation regions are found in the skippable last three blocks and they are gradually concentrated around the target object, demonstrating the refinement of learned features. While ResNet50-ADN(TTTT), or base-net, shares the parameters with the super-net’s. This is because while the super-net and the base-net share parameters in the non-skippable mandatory blocks, they use different batch normalization operators in the mandatory sub-paths. Further, in Figure 8-(c), we can observe that the final activation map of the base-net is very similar to the super-net’s final activation map in Figure 8-(b). This implies that they have similar distributions for the same inputs, as suggested in Section 3.3.

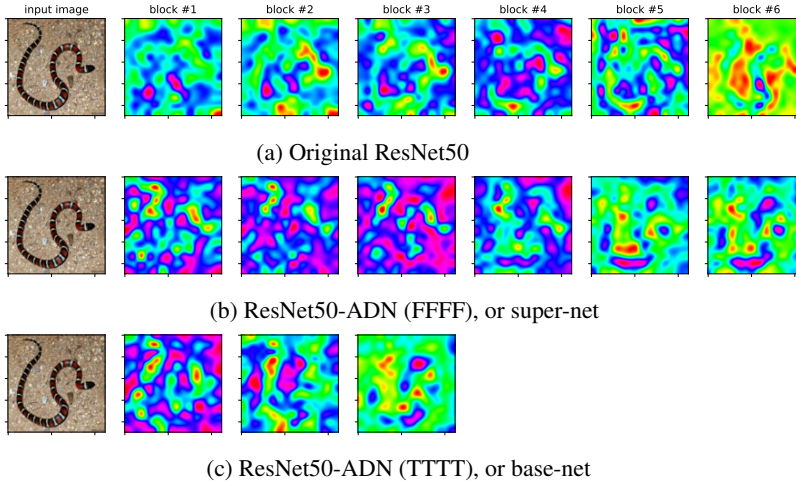


Figure 8: Class Activation Maps of the 3rd residual stages of ResNet50s. **(a)** Original ResNet50’s activation regions change gradually across all blocks. **(b)** In ResNet50-ADN (super-net), the first 3 blocks have extensive hot activation regions, implying active learning of new level features. In contrast, the skippable last 3 blocks have far less activation regions and they are gradually refined around the target. **(c)** Even though parameters are shared, the activation map of base-net is very different from super-net’s since they use different batch normalization operators.